Available online at www.sciencedirect.com
SCIENCE DIRECT®
Journal of Asian Earth Sciences 23 (2004) 799–813
Journal of Asian Earth Sciences
www.elsevier.com/locate/jseaes

Continental crustal growth and the supercontinental cycle: evidence from the Central Asian Orogenic Belt

Dawei Hong[a,*], Jisheng Zhang[a], Tao Wang[a], Shiguang Wang[b], Xilin Xie[c]

[a]*Institute of Geology, Chinese Academy of Geological Sciences, Beijing 100037, China*
[b]*Department of Geology, Peking University, Beijing 100871, China*
[c]*Institute of Mineral Deposits, Chinese Academy of Geological Sciences, Beijing 100037, China*

Abstract

Studies of supercontinental cycle are mainly concentrated on the assembly, breakup and dispersal of supercontinents, and studies of continental crustal growth largely on the growth and loss (recycling) of the crust. These two problems have long been studied separately from each other. The Paleozoic–Mesozoic granites in the Central Asian Orogenic Belt have commonly positive εNd values, implying large-scale continental crustal growth in the Phanerozoic. They coincided temporally and spatially with the Phanerozoic Pangea supercontinental cycle, and overlapped in space with the *P*-wave high-*V* anomalies and calculated positions of subducted slabs for the last 180 Ma, all this suggests that the Phanerozoic Laurasia supercontinental assembly was accompanied by large-scale continental crustal growth in central Asia. Based on these observations, this paper proposes that there may be close and original correlations between a supercontinental cycle, continental crustal growth and catastrophic slab avalanches in the mantle. In this model we suggest that rapid continental crustal growth occurred during supercontinent assembly, whereas during supercontinental breakup and dispersal new additions of the crust were balanced by losses, resulting in a steady state system. Supercontinental cycle and continental crustal growth are both governed by changing patterns of mantle convection.

Keywords: Continental crustal growth; Supercontinent; Central Asian Orogenic Belt

1. Introduction

Supercontinental cycle and continental crustal growth are undoubtedly two of the most important subjects of research and debate in the earth sciences today. The study of the former is mainly concentrated on the assembly, breakup and dispersal of supercontinents, and the study of the latter largely on the growth and loss (recycling) of the crust. These two problems have long been studied separately from each other. However, it has been recognized that they are both related to the changing patterns of mantle convection (Hoffman, 1989; Stein and Hofmann, 1994; Condie, 1998). If so, how are the changing patterns of mantle convection related to the supercontinental cycle and continental crustal growth, and how is the supercontinental cycle related to continental crustal growth?

There is a growing consensus that at several times in the history of the earth most or all the continents have gathered to form one or two supercontinents, which later split into many smaller continents only to rejoin and form a supercontinent again. A supercontinent is defined on completion of its assembly and suturing events. The recognized periods of supercontinental accumulation were broadly at about 2600, 1800, 1000, 650, and 250 Ma ago (Nance et al., 1988; Hoffman, 1992).

Two major hypotheses have been proposed to explain continental crustal growth (Fig. 1). The first proposes that the present mass of the crust was formed very early in earth history and has been recycled through the mantle in steadily decreasing fashion such that new additions are balanced by losses, resulting in a steady state system (Armstrong, 1968; Bowring and Housh, 1995). The second proposes that the crust grew throughout geological time, with variations from a steady rate to growth in major episodic pulses. These episodes of crustal growth generally occurred at about 3.6–3.5, 2.7–2.6, 2.0–1.8, 1.2–1.0, and 0.5–0.3 Ga (McCulloch and Bennett, 1994; Taylor and McLennan, 1995; Condie, 1998).

Therefore, apart from the early Archean, the episodes of crustal growth appear to correlate reasonably well with supercontinental assembly phases, which indicate that

* Corresponding author.
E-mail address: hongdw@cags.cn.net (D. Hong).

1367-9120/03/$ - see front matter © 2003 Elsevier Ltd. All rights reserved.
doi:10.1016/S1367-9120(03)00134-2

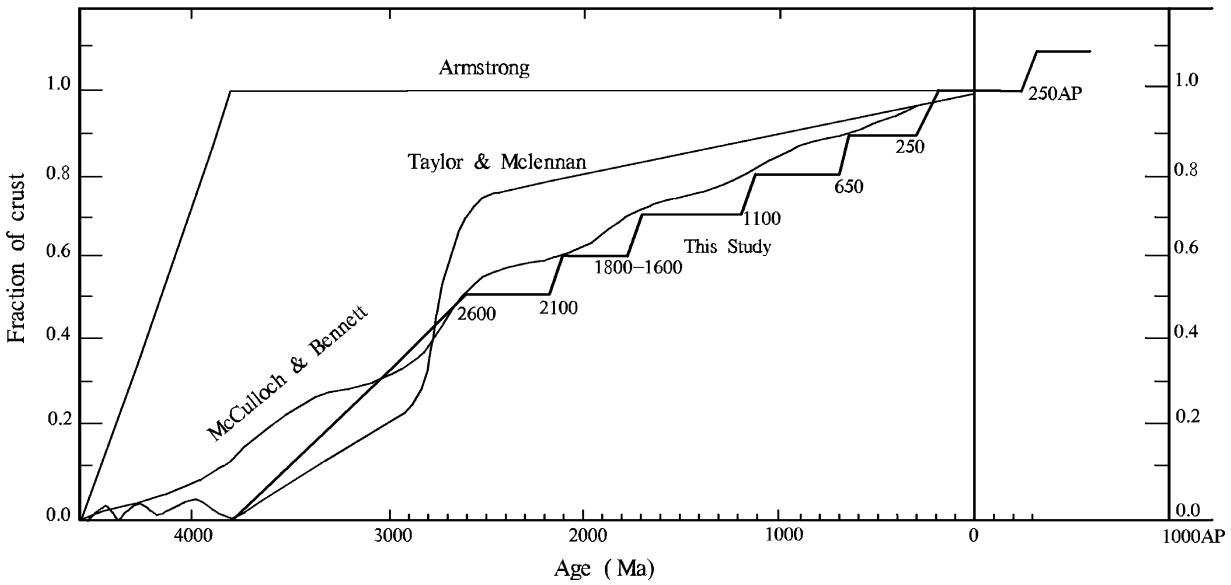

Fig. 1. A selection of crustal growth models. Models shown are those of Armstrong (1968); McCulloch and Bennett (1994); Taylor and McLennan (1995), and this paper.

supercontinental cycles likely have an important convection with crustal evolution (Taylor and McLennan, 1995). Condie (1998, 2000) suggested that each maximum in continental growth was interpreted to reflect a supperplume event in the mantle caused by catastrophic slab avalanching at 660 km discontinuity, whereas the supercontinent cycle probably operates independently of slab avalanches. Crustal recycling rate may drop significantly below crustal production rate during slab avalanches due to the formation of supercontinents, which trap juvenile crust. Supercontinents are responsible for the preservation of large amounts of juvenile crust, and play an important role in the growth of continental crust with time. Based on the research of granites with positive εNd values from the Central Asian Orogenic Belt, Hong et al. (2001) proposed that the supercontinental cycle could be related closely to continental crustal growth. The time periods when large areas of continental crust were rapidly formed during supercontinental assembly alternated with apparently more quiescent periods of low-crust-forming rates during supercontinental breakup and dispersal. It is the purpose of this short contribution to speculate further on the correlation between the supercontinental cycle, continental crustal growth in earth history and changing patterns of mantle convection.

2. Sm–Nd isotopic characteristics of the granites in the CAOB

The Central Asian Orogenic Belt (CAOB) is bounded by the Siberian and Sino-Korean-Tarim cratons (Fig. 2). The Paleo-Asian ocean, which provided the framework for the CAOB, was opened by 1020 Ma (Khain et al., 2002), and its maximum opening occurred after or simultaneously with the first accretion–collision event at 600–700 Ma, resulting from the collision of microcontinents and the Siberian continent. The final closure of the Paleo-Asian ocean occurred in the late Devonian–early Carboniferous (Dobretsov et al., 1995).

The CAOB is characterized by very large volumes of granitic rocks emplaced from the early Paleozoic to late Mesozoic, occupying a total area more than 5,000,000 km^2. The available geochronology of granites shows that granitic magmatism began before about 500 Ma, and reached the peak during the final closure of the Paleo-Asian ocean and the collision between the Siberian and Sino-Korean-Tarim plates at the late Devonian–early Carboniferous, and continued during the extensional regime after the collision event (Hong et al., 2000). The granites thus define tectonic settings from subduction type through collision type to post-collisional extensional type. Extensive I-type, S-type and A-type granites are therefore present in this region.

Based on available Sm–Nd isotopic data on the granites from eastern Kazakhstan, Altai, eastern and western Junggar, Alatao mountains, Tianshan mountains, Xinjiang, China, Mongolia, Transbaikalia, Russia, Inner Mongolia, China, northeastern China and Sikhote Alin, Russia (Table 1), some general characteristics can be summarized as follows:

(1) The voluminous granites are characterized by positive εNd(T) values with limited variation, regardless of the intrusive age (early and late Paleozoic, and Mesozoic), tectonic settings (syn-, late-, post-, and anorogenic) and granite type (I-, S-, A-, and M-type). This feature indicates that there is little correlation between Nd isotope signature and bulk composition, which in turn suggests restricted contribution of the ancient crustal material (Fig. 3). They are quite similar to contemporaneous

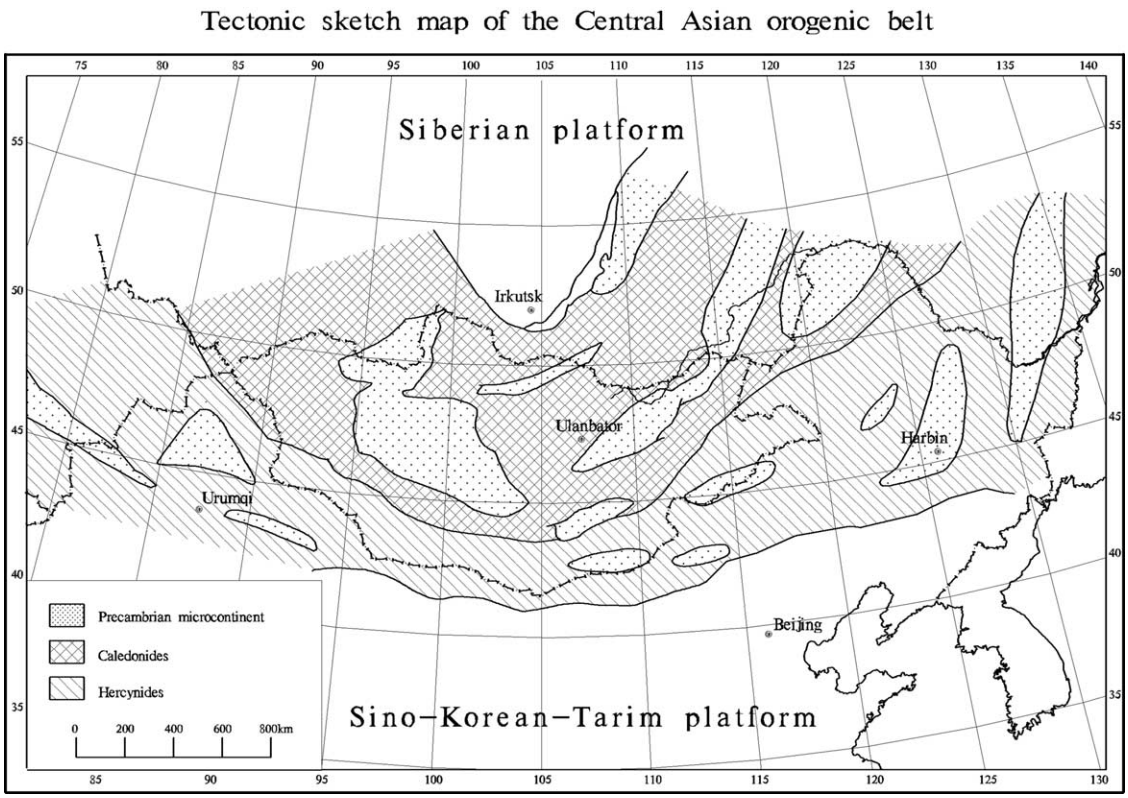

Fig. 2. Tectonic sketch map of the Central Asian Orogenic Belt.

basic-ultrabasic rocks, but different from the Phanerozoic granites from the Caledonian, Hercynian and Himalayan orogenic belts, and the S-type and I-type granites from the Lachlan fold belt, Australia (Fig. 3).

Continental crust is commonly classified as either juvenile (mantle-derived) or evolved (derived at least in part from older enriched crust) on the basis of initial Nd isotopic compositions. Positive εNd is considered to reflect derivation from juvenile sources, whereas negative εNd is interpreted to reflect derivation from evolved sources (Bowring and Housh, 1995). Hence, the sources of the granites with positive εNd values in the CAOB were documented by juvenile material derived from the depleted mantle, which contrasts with other Phanerozoic crust-derived granites characterized by negative εNd values.

The generation of voluminous, compositionally evolved, magmas with sources dominated by depleted mantle-like materials raises obvious petrogenetic questions, but this does not have to be a single-stage process. Both assimilation-fractional crystallization (AFC) models (De Paolo, 1981) and melting–assimilation–storage–homogenization (MASH) models (Hildreth and Moorbath, 1988) can be extended to allow remelting and assimilation of juvenile addition to the crust by successive magma batches over short time scale.

(2) The T_{DM} values of granites, regardless of their intrusive ages, vary in the range of 500–1000 Ma, with a peak at 700–800 Ma (Fig. 4). Compared with other Phanerozoic granites over the world, they show relatively younger T_{DM} values with limited variation. This could indicate the isotopic homogeneity of sources. However, the Nd model ages for the examined granites appear to be older than the crystallization ages of the oldest granitoids (520 Ma, Kovalenko et al., 1996a). This suggests that some old crustal material was involved in the granite petrogenesis.

(3) Only those granites which intruded into the Precambrian microcontinents, most of which are younger than 300 Ma, show negative εNd values, older $T_{DM,}$ and remarkable scatter of their εNd and T_{DM} values over the interval between ~200 and ~300 Ma (Kovalenko et al., 1996a; Hong et al., 2000). This scatter suggests that the sources of the granites in microcontinents were isotopically heterogeneous. But compared with other typical Phanerozoic crust-derived granites over the world, they have higher εNd values and lower T_{DM}. This feature might suggest that old Precambrian crust was actively involved in the petrogenesis of the granites since about 300 Ma. The data also suggest that the source of granites was still dominated by juvenile mantle material. This is consistent with the general characteristics of the granites in the CAOB.

(4) εNd values of granites gradually decreased with the decreasing age of the granites, showing a clear evolution trend of Nd isotopic composition. Particularly, Mesozoic granites younger than 200 Ma are characterized by εNd values approaching zero, a common feature for granites in

Table 1
Sm–Nd isotope data of the granites in the Central Asian Orogenic Belt

Location	Rock type (number of sample)	Age (Ma)	εNd(*T*)	T_{DM} (Ma)	Reference
Central Kazakhstan					
Aksu	Quartz monzodiorite (2)	450	3.49–3.53	789–756	Heinhorst et al. (2000)
	Porphyritic granodiorite (2)	450	3.13–3.12	744–746	Heinhorst et al. (2000)
	Hornblende gabbro (1)	450	2.83	814	Heinhorst et al. (2000)
	Granite (1)	450	2.82	748	Heinhorst et al. (2000)
Stepnyak	Hornblende gabbro (1)	450	0.04	1208	Heinhorst et al. (2000)
	Quartz monzodiorite (1)	450	−0.76	1167	Heinhorst et al. (2000)
Dollinye	Gabbro (1)	300	5.54	563	Heinhorst et al. (2000)
	Porphyritic granodiorite (1)	300	4.52	583	Heinhorst et al. (2000)
	Porphyritic monzodiorite (1)	300	5.54	522	Heinhorst et al. (2000)
	Quartz diorite (2)	300	4.95–5.32	565–539	Heinhorst et al. (2000)
Aqtogay	Porphyritic granodiorite (1)	300	5.58	498	Heinhorst et al. (2000)
	Granodiorite (1)	300	4.45	603	Heinhorst et al. (2000)
	Granite (1)	300	5.41	508	Heinhorst et al. (2000)
	Porphyry stock (1)	300	2.86	672	Heinhorst et al. (2000)
	Granophyre (1)	300	5.94	403	Heinhorst et al. (2000)
Kounrad	Hornblende granodiorite (1)	325	0.72	828	Heinhorst et al. (2000)
Nurataldy	Leucogranite (2)	330	2.03–0.88	684–797	Heinhorst et al. (2000)
Aqshatau	Leucogranite (2)	285	0.75 to −3.03	658–1010	Heinhorst et al. (2000)
Batystau	Leucogranite (2)	310	−0.59 to −0.43	818–753	Heinhorst et al. (2000)
Bektauata	Leucogranite (1)	290	0.89	890	Heinhorst et al. (2000)
Kounrad East	Aplite (1)	295	1.62	572	Heinhorst et al. (2000)
Verkhnee Espe	Riebeckite granite (4)	250	5.28–7.86	243–391	Heinhorst et al. (2000)
Altai, Russia					
Chindagatui	Leucogranite (4)	200	−3.29 to −4.99		Vladimirov et al. (1998)
Kungurdzharin	Leucogranite (2)	200	−2.33 to −2.53		Vladimirov et al. (1998)
Gorny Schoriya and northern Gorny Altai	Granitoids	Early Cambrian–early Triassic	5.8–0.9	780–940	Kruk et al. (1999)
					Kruk et al. (1999)
Mineral Altai	Granitoids (1)	Permian-Triassic	2.1	950	Kruk et al. (1999)
Southern Gorny Altai	Granitoids	Mid-Paleozoic-early Devonian	−1.3 to −4.7	1190–390	Kruk et al. (1999)
					Kruk et al. (1999)
Northwestern Gorny Altai	Granitoids	Late Devonian–early Carboniferous	−0.7–1.1	1050–1200	Kruk et al. (1999)
Altai, Xinjiang, China					
Heishantou	Granite (1)	270	8.3	360	Hong Dawei et al. unpublished data
Buerjin	Porphyritic granite (1)	275	2.57	830	Hong Dawei et al. unpublished data
Haliutan	Monzogranite (1)	296	−1.13	1150	Hong Dawei et al. unpublished data
Hanasi	Granite (2)	290	−0.77 to −2.52	1120–1260	Hong Dawei et al. unpublished data
Erkuangdaqiao	Gneissic granite (1)	360	1.12	1020	Hong Dawei et al. unpublished data
Dahalasu	Granite (3)	255	1.28–7.00	460–920	Hong Dawei et al. unpublished data
Shangkelan	Mica granite (1)	181	2.42	840	Hong Dawei et al. unpublished data
Aweitan	Granite (1)	296	2.13	890	Hong Dawei et al. unpublished data
Keketuohai	Granite (1)	399	−5.65	1600	Hong Dawei et al. unpublished data
Keketuohai south	Granite (1)	388	−0.89	1210	Hong Dawei et al. unpublished data
Furen	Granite (1)	275	5.62	590	Hong Dawei et al. unpublished data
Aierdengbulake	Hornblende monzogranite (4)	292	5.38–6.97	490–620	Hong Dawei et al. unpublished data
	Diabase (1)	292	4.78	430	Hong Dawei et al. unpublished data
Bielatubiekuduke	Diorite (1)	292	5.78	590	Hong Dawei et al. unpublished data
Aletai	Granite (1)	330	−2.0	1290	Chen et al. (2001)
Keketuohai	Granite (2)	390	−0.6 to −2.6	1140–1530	Chen et al. (2001)
Qiemaiqieke	Gneissic granite (2)	290	−1.98–0.80	1062–1096	Zhao et al. (1993)
Wuqiliketawu	Granite (1)	290	−1.39	1417	Zhao et al. (1993)
Keketuohaibei north	Granite (1)	330	0.45	1059	Zhao et al. (1993)
Tabieqi	Granite (1)	290	1.33	998	Zhao et al. (1993)
Jiamukai (Daqiao)	Granite (1)	290	−5.34	1458	Zhao et al. (1993)
Halaayijuehuo	Quartz diorite (1)	290	−0.55	1356	Zhao et al. (1993)

(*continued on next page*)

Table 1 (*continued*)

Location	Rock type (number of sample)	Age (Ma)	εNd(*T*)	T_{DM} (Ma)	Reference
Kangbutiebao	Granite (1)	290	1.73	771	Zhao et al. (1993)
Hill 60	Mica granite (1)	290	−3.85	1166	Zhao et al. (1993)
Habahe	Granite (1)	290	1.21	775	Zhao et al. (1993)
Hanasi	Granite (1)	290	−2.87	1355	Zhao et al. (1993)
Jiangjunshan	Amazonite-bearing granite (2)	290	2.14–2.46	976–1008	Zhao et al. (1993)
Qinggeli	Tonalite–granodiorite (1)	408	0.48	1002	Zhao et al. (1993)
Dahe	Tonalite–granodiorite (1)	408	0.22	1112	Zhao et al. (1993)
Hemu	Tonalite–granodiorite (1)	408	0.65	1015	Zhao et al. (1993)
Tuergun	Monzogranite (1)	377	−1.58	1378	Zhao et al. (1993)
Asele	Dacite porphyry (2)	296	2.50–4.4	1210–1715	Li et al. (1998)
	Sub-rhyolite porphyry (2)	294	3.57–4.35	1404–1484	Li et al. (1998)
	Jaspilite (5)	378	1.52–1.9		Li et al. (1998)
	Spilite (6)	360	6.7–8.1		Li et al. (1998)
Habahe	Granodiorite (2)	360	0.9–1.2	1210–1040	Li et al. (1998)
Suoerkuduke	Altered andesite (2)	288	5.4–5.9		Li et al. (1998)
Kalatongke	Basic-ultrabasic rocks (6)	298	5.94–6.08	596–650	Li et al. (1998)
West Zhungaer, Xinjiang, China					
Longleinuohai	Plagiogranite (1)	523	6.43	716	Zhao et al. (1996)
Tangbale	Plagiogranite (1)	500	4.88	1126	Zhao et al. (1996)
Dalabute	Plagiogranite (1)	395	7.8	353	Zhao et al. (1996)
Buerkesidai	Diabase porphyry (1)	329	6.06	654	He et al. (1994)
	Alkali-feldspar granite (1)	314	5.65	540	He et al. (1994)
Kelamayi east	Monzogranite (1)	320	6.00–6.10	456–561	Kwon et al. (1989)
Kelamayi west	Hypersthene granite	320	4.8–5.9	690–790	Sun et al. (1998)
	Enclave	320	2.6–3.5		Sun et al. (1998)
	Peralkaline granite	280	5.0–5.8		Sun et al. (1998)
East Zhungaer, Xinjiang, China					
Hongtujingzi	Monzogranite (2)	300	5.84–7.51	450–590	Hong Dawei et al. unpublished data
Kamusite	Monzogranite (2)	276.6	5.42–8.52	350–600	Hong Dawei et al. unpublished data
Beilekuduke	Syenogranite (1)	313	6.59	540	Hong Dawei et al. unpublished data
Laoyaquan	Monzogranite (1)	300	6.79	550	Hong Dawei et al. unpublished data
Saruoshike	Peralkaline granite (3)	290	3.73–7.31	460–750	Hong Dawei et al. unpublished data
Yushugou	Peralkaline granite (5)	300	4.09–8.45	370–730	Hong Dawei et al. unpublished data
	Granite porphyry (1)	300	6.79	510	Hong Dawei et al. unpublished data
Dajiashan	Peralkaline granite (6)	276	6.18–9.51	430–540	Hong Dawei et al. unpublished data
	Syenogranite (1)	276	6.24	540	Hong Dawei et al. unpublished data
Saerbulake	Diorite (1)	290	5.18	668	Zhao et al. (1996)
Buergen	Granodiorite (1)	290	3.42	792	Zhao et al. (1996)
	Syenogranite (1)	250	1.40	733	Zhao et al. (1996)
	Peralkaline granite (1)	250	0.62	1029	Zhao et al. (1996)
Ertai	Alkaline gabbro (1)	290	7.27	514	Zhao et al. (1996)
	Peralkaline syenite (1)	290	−3.81	1335	Zhao et al. (1996)
Jieerdakala	Peralkaline granite (1)	300	6.09–6.67	523–557	Han et al. (1997)
Sawydegeer	Peralkaline granite (1)	300	5.56–6.47	501–606	Han et al. (1997)
Saertielieke	Peralkaline granite (1)	300	5.12–5.61	692–1003	Han et al. (1997)
South-Tasigake	Peralkaline granite (1)	300	5.06–5.54	570–878	Han et al. (1997)
Yebushan	Syenogranite (5)	267	5.51–5.84	591–694	Han et al. (1998)
Hongtujingzi-kamosite	Tonalite–Trondjemite (1)	316	9		Hopson et al. (1989)
	Granodiorite–granite	300	7		Hopson et al. (1989)
Armantai	Gabbro	561	6.1		Huang et al. (1997)
Alatao Mountains, Xinjiang, China					
Kongwusayi	Syenogranite (1)	290	2.80	926	Zhou et al. (1996)
Wulasitan	Granodiorite (1)	290	2.76	1165	Zhou et al. (1996)
Zuluhong	Monzogranite (1)	290	3.14	1206	Zhou et al. (1996)
Kazibieke	Syenogranite (1)	290	2.17	1131	Zhou et al. (1996)
Chaganhundi	Syenogranite (1)	290	2.43	962	Zhou et al. (1996)

(*continued on next page*)

Table 1 (*continued*)

Location	Rock type (number of sample)	Age (Ma)	εNd(*T*)	T_{DM} (Ma)	Reference
Tianshan mountains, Xinjiang, China					
Eastern North Tianshan mountains	Granodiorite (1)	345	5		Hopson et al. (1989)
Eastern Central Tianshan mountains	Granite (1)	334–261	4		Hopson et al. (1989)
Korla, Eastern South Tianshan mountains	Granite (1)	Early Carboniferous	−8		Hopson et al. (1989)
Qiaoletiekexi, west Tianshan mountains	Gabbro (1)	324	3.68	1907	Ni et al. (1994)
Qiongawuzi, west Tianshan mountains	Gabbro (1)	314	−5.07	1585	Ni et al. (1994)
Sulu, west Tianshan mountains	Gabbro (1)	322	6.40	1964	Ni et al. (1994)
Qingbulake, west Tianshan mountains	Olivin-gabbro (1)	320	3.79	1051	Ni et al. (1994)
	Pyroxenite (1)	320	3.87	1058	Ni et al. (1994)
Kaladala, west Tianshan mountains	Olivin-gabbro (1)	320	6.00	842	Chen et al. (1995)
Qiulaketeleke, west Tianshan mountain	Diabase (1)	320	1.68	891	Chen et al. (1995)
Nileke, west Tianshan mountain	Basalt (2)	298	3.5–5.8		Li et al. (1998)
	Quartz albite porphyry (2)	247	0.8–0.9		Li et al. (1998)
Kangguertage, east Tianshan mountain	Altered andesite (2)	290	2.6–3.2		Li et al. (1998)
	Altered rhyolite (2)	300	0.2–0.6		Li et al. (1998)
	Tonalite (2)	248	0.3–3.6		Li et al. (1998)
Huangshan, east Tianshan mountain	Basic-ultrabasic rocks (8)	308	6.6		Li et al. (1998)
East Huangshan, east Tianshan mountain	Basic-ultrabasic rocks (6)	320	7.8		Li et al. (1998)
Tuwu, east Tianshan mountain	Rhyolite (1)	416	5.6		Rui et al. (2002)
	Dacite (1)	416	8.8		Rui et al. (2002)
	Andesite (1)	416	8.8		Rui et al. (2002)
	Basalt-trachyte (2)	416	8.0–8.3		Rui et al. (2002)
	Trachyte–andesite-basalt (2)	416	8.2–8.6		Rui et al. (2002)
	Altered plagiogranite porphyry (7)	369	6.2–9.4		Rui et al. (2002)
Mongolia					
Caledonian orogenic belt in north-central Mongolia	Granitoids (2)	122–126	0.7–1.9	786–833	Kovalenko et al. (1996a)
	Granitoids (4)	190–230	1.3–2.2	824–915	Kovalenko et al. (1996a)
	Granitoids (2)	300–320	2.0–2.7	872–915	Kovalenko et al. (1996a)
	Granitoids (4)	360–390	2.8–7.0	575–906	Kovalenko et al. (1996a)
	Granitoids (4)	400–450	4.6–7.9	583–868	Kovalenko et al. (1996a)
	Granitoids (8)	530–570	6.7–9.9	481–718	Kovalenko et al. (1996a)
Late-Proterozoic microcontinents in the Caledonides	Granitoids (2)	123–128	−2.5 to −4.3	1145–1304	Kovalenko et al. (1996a)
	Granitoids (8)	188–230	−1.9–0.6	892–1174	Kovalenko et al. (1996a)
	Granitoids (7)	253–300	−7.5 to −1.6	1183–1715	Kovalenko et al. (1996a)
	Granitoids (2)	360–390	−2.0–0.1	1174–1300	Kovalenko et al. (1996a)
Hercynian orogenic belt in south Mongolia	Granitoids (8)	260–320	3.5–9.4	304–764	Kovalenko et al. (1996a)
Late-Proterozoic microcontinents in the Hercynides	Granitoids (2)	156–157	0.8–1.3	860–900	Kovalenko et al. (1996a)
	Granitoids (3)	200	0.2–1.4	885–987	Kovalenko et al. (1996a)
	Granitoids (4)	280–300	−3.2–1.4	860–1336	Kovalenko et al. (1996a)

(*continued on next page*)

Table 1 (*continued*)

Location	Rock type (number of sample)	Age (Ma)	εNd(*T*)	T_{DM} (Ma)	Reference
Khaldzan-Buregtey, Kobdo, west Mongolia	Nordmakite (1)	378	2.76	910	Kovalenko et al. (1992)
	Peralkaline granite (4)	378	5.80–7.67	530–660	Kovalenko et al. (1992)
	Bearing rare metal peralkaline granite (6)	378	4.33–5.70	690–780	Kovalenko et al. (1992)
	Granite (1)	378	2.66	910	Kovalenko et al. (1992)
	Pantellerite (4)	378	4.78–5.62	700–750	Kovalenko et al. (1992)
	Leucite basalt (1)	378	4.33	530	Kovalenko et al. (1992)
	Dolerite	378	2.76	910	Kovalenko et al. (1992)
Seriin-Huru, west Mongolia	Gabbro (3)	527	6.6–7.0		Kovalenko et al. (1996b)
	Basalt (4)	527	7.0–9.8		Kovalenko et al. (1996b)
Geriin-Huru, west Mongolia	Basalt (1)	522	8.0		Kovalenko et al. (1996b)
Proterozoic Dzabkhan microcontinent in the Caledonides, central Mongolia	Biotite granite (1)	300	−7.6	1469	Kozakov et al. (1997)
	Biotite granite (1)	500	−4.1	1333	Kozakov et al. (1997)
	Biotite granite (1)	280	−2.7	1330	Kozakov et al. (1997)
Bayan-Khongor ophiolite in the Caldonides, central Mongolia	Gabbro (1)	569	11.9		Kepezhinskas et al. (1991)
Goby-Altai zone central Mongolia	Basalt (6)	270	0.2–5.9	560–1020	Yarmolyuk et al. (1997)
Dzanchivelan, central Mongolia	Bearing rare metal Li–F granite (5)	195	0.5–1.2	892–953	Kovalenko et al. (1999)
Baga-Gazrin, central Mongolia	Bearing rare metal Li–F granite (1)	202	1.9	846	Kovalenko et al. (1999)
Borun-tsogtin, east Mongolia	Bearing rare metal Li–F granite (1)	128	1.8	789	Kovalenko et al. (1999)
Southdzir, east Mongolia	Bearing rare metal Li–F granite (2)	284	1.3–2.3	877–954	Kovalenko et al. (1999)
	Bearing rare metal Li–F granite (2)	200	0.2	987	Kovalenko et al. (1999)
	Bearing rare metal Li–F granite (1)	157	0.8–1.2	861–900	Kovalenko et al. (1999)
Goby-Tianshan mountains zone, south Mongolia	Basalt (6)	290	2.2–8.1	400–880	Yarmolyuk et al. (1997)
South Khangai, south Mongolia	Nephelinite (1)	150	1.2		Yarmolyuk et al. (1995)
	Basalt (4)	103–133	−0.1–3.6		Yarmolyuk et al. (1995)
	Basanite (1)	75	4.6		Yarmolyuk et al. (1995)
	Basalt (2)	34–47	−10.7–34.8		Yarmolyuk et al. (1995)
	Tephrite (1)	26	−2.6		Yarmolyuk et al. (1995)
	Basalt (2)	14	−9.2		Yarmolyuk et al. (1995)
	Basanite (1)	9.9	−10.7		Yarmolyuk et al. (1995)
	Basalt (3)	3.6–8.9	1.2–4.8		Yarmolyuk et al. (1995)
	Basanite (1)	1.2	−2.1		Yarmolyuk et al. (1995)
North Mongolia-Transbaikalia	Basalt (7)	250	−0.5–1.6	890–1060	Yarmolyuk et al. (1997)
Transbaikalia, Russia					
Betsimyan	Amazonite granite (1)	265	−6.9	1534	Kovalenko et al. (1999)
Haragul	Amazonite granite (3)	317	−1.2 to −2.7	1066–1330	Kovalenko et al. (1999)
Orlov	Amazonite granite (2)	142	0.1		Kovalenko et al. (1999)
Hangilai	Amazonite granite (1)	142	−1.3		Kovalenko et al. (1999)
Soktui	Biotite granite (1)	142	−0.01		Kovalenko et al. (1999)
Atinkin	Amazonite granite (1)	142	1.4		Kovalenko et al. (1999)
Ari-Bulak	Ongonite (2)	142	−0.9 to −1.7		Kovalenko et al. (1999)

(*continued on next page*)

Table 1 (*continued*)

Location	Rock type (number of sample)	Age (Ma)	εNd(*T*)	T_{DM} (Ma)	Reference
Malo-Khamardaban	Tephrite-basalt (5)	140–153	−2–1.1		Yarmolyuk et al. (1998)
	Basalt-tephrite–teschenite (6)	102–136	−1–2.1		Yarmolyuk et al. (1998)
Khilok	Basalt-tephrite (9)	80–135	−2.0–1.7		Yarmolyuk et al. (1998)
	Basalt-basanite (5)	27–48	−2.1–5.1		Yarmolyuk et al. (1998)
Udino-Vitim	Tephrite–trachyte-basalt (3)	144–170	−0.6–0.3		Yarmolyuk et al. (1998)
	Basalt-tephrite–basanite (4)	70–124	−1.7–3.6		Yarmolyuk et al. (1998)
	Basalt-basanite (4)	1–50	1.1–4.2		Yarmolyuk et al. (1998)
Bryan	Peralkaline granite (2)	275	−2.9 to −2.5		Yarmolyuk et al. (2001)
	Subalkaline granite (3)	275	−2.3 to −3.4		Yarmolyuk et al. (2001)
	Comendite (2)	275	−2.6 to −3.2		Yarmolyuk et al. (2001)
Thagan-Khurteik	Basalt (4)	209	0.8–2.8		Yarmolyuk et al. (2001)
	Trachyte (1)	209	1.8		Yarmolyuk et al. (2001)
	Comendite (3)	209	2.1–2.6		Yarmolyuk et al. (2001)
Kharitonov	Alkaline syenite (1)	209	−1.2		Yarmolyuk et al. (2001)
	Peralkaline granite (1)	209	−4.2		Yarmolyuk et al. (2001)
	Comendite (2)	210	−1.5 to −1.6		Yarmolyuk et al. (2001)
	Basalt (3)	209	0.8–2.5		Yarmolyuk et al. (2001)
Ddzida river	Basalt (2)	102–109	2–2.1		Vorontsov et al. (2002)
	Teschenite (1)	109	1.4		Vorontsov et al. (2002)
	Tephrite (2)	125–132	−1–0.1		Vorontsov et al. (2002)
	Basalt (1)	136	0.5		Vorontsov et al. (2002)
	Tephrite (2)	140–150	0–1.1		Vorontsov et al. (2002)
	Tephrite (1)	153	−2		Vorontsov et al. (2002)
	Basalt (2)	145–150	−1.4 to −2.0		Vorontsov et al. (2002)
Solonker zone, Central Inner Mongolia, China					
Baiyinwula	Peralkaline granite (3)	286	3.6–5.7	520–701	Hong Dawei et al. unpublished data
Zanawula	Peralkaline granite (4)	277	2.63–6.18	490–744	Hong Dawei et al. unpublished data
Zuhengdeleng	Peralkaline granite (5)	284	1.17–6.49	520–1008	Hong Dawei et al. unpublished data
Narenbaolige	Peralkaline granite (4)	277	2.75–5.03	410–590	Hong Dawei et al. unpublished data
Shaerhada	Peralkaline granite (1)	277	2.38	620	Hong Dawei et al. unpublished data
Proterozoic Xilinhot microcontinent in the Hercynides, Central Inner Mongolia, China					
Sonidzuoqi	Mica granite (1)	206	0.9	910	Hong Dawei et al. unpublished data
Wulayintuiraomu	Biotite syenogranite 1)	152	2.03	780	Hong Dawei et al. unpublished data
Zhunhubeeryinhuduge	Biotite monzogranite (1)	206	−0.25	1010	Hong Dawei et al. unpublished data
Gaoleyinhudugewula	Mica granite (1)	206	−2.98	1230	Hong Dawei et al. unpublished data
Wadengyingele	Syenogranite (1)	216	−1.21	1090	Hong Dawei et al. unpublished data
Bagageeryinzhusilang	Syenogranite (2)	216	−0.73–1.84	850–1050	Hong Dawei et al. unpublished data
Adunchulu	Syenogranite (1)	216	1.69	860	Hong Dawei et al. unpublished data
Bagaaobao	Syenogranite (1)	136	−2.34	1120	Hong Dawei et al. unpublished data
Chagandeersi	Monzogranite (1)	136	−4.95	1220	Hong Dawei et al. unpublished data
Yamaqi	Biotite granite (1)	110	−1.94	1070	Hong Dawei et al. unpublished data
Berenaobao	Monzogranite (3)	231	2.09–2.65	790–840	Hong Dawei et al. unpublished data
Gasimaodeng	Syenite (3)	297	5.52–5.82	560–590	Hong Dawei et al. unpublished data
Xianghuangqi	Monzogranite (4)	261	−5.31 to −7.01	1460–1510	Hong Dawei et al. unpublished data
Taigushengmiao	Monzogranite (4)	277	−6.51–0.84	960–1570	Hong Dawei et al. unpublished data
Bainaimiao	Amphiubole granite (4)	459	−2.63 to −4.21	1410–1540	Hong Dawei et al. unpublished data
	Quartz diorite (3)	454	−1.36 to −3.78	1300–1500	Hong Dawei et al. unpublished data
Baolidao	Gabboric diorite (7)	310	−0.2–2.4	890–1110	Chen et al. (2000)
Halatu	Granite (6)	230	−2.2–1.0	940–1210	Chen et al. (2000)
South Xinggan mountains, Inner Mongolia, China					
Barzhe	Peralkaline granite (6)	125	1.93–2.50	710–759	Wang et al. (1997)
Biliutai	Qrthoclase syenogranite (7)	200	3.21–4.80	610–790	Zhu et al. (2001)
Baitazi	Syenogranite (1)	115	1.93	1020	Shao et al. (1999)
	Porphyritic granodiorite (1)	117	0.82	850	Shao et al. (1999)
Laoshenfang	Porphyritic syenogranite (1)	127	0.82	820	Shao et al. (1999)
	Granodiorite (1)	136	1.35	860	Shao et al. (1999)
Jiulianshan	Monzogranite (1)	137	1.60	470	Shao et al. (1999)
Laoheishan	Granodiorite (1)	213	1.47	870	Shao et al. (1999)
Shuguang	Mica granite (1)	242	2.17	840	Shao et al. (1999)

(*continued on next page*)

Table 1 (*continued*)

Location	Rock type (number of sample)	Age (Ma)	εNd(*T*)	T_{DM} (Ma)	Reference
Zhelimumeng	Basalt-latite–trachyte (2)	121	3.8–3.3		Shao et al. (1999)
Lindong	Pyroxene andesite, trachytic andesite (2)	142	0.39–0.40		Shao et al. (1999)
Lubei	Trachyte–dacite, rhyolite, andesite (5)	121	1.05–3.88	605–897	Chen et al. (1997)
Tianshan	Rhyolite, trachytic dacite	142	−3.02–3.73	667–1260	Chen et al. (1997)
West Inner Mongolia, China					
Yagan	Garnet monzogranite (1)	228	−0.8	2250	Wang et al. (2004)
	Monzogranite (4)	228	−1.3 to −2.3	960–1070	Wang et al. (2004)
	Granodiorite (1)	135	−1.5	960	Wang et al. (2004)
	Biolite monzonite (1)	135	5.2	640	Wang et al. (2004)
	Monzogranite (1)	135	0.5	1490	Wang et al. (2004)
	Enclave (1)	135	1.2	640	Wang et al. (2004)
Northeast China					
Boketou	Tonalite (1)	156	0.48	904	Wu et al. (2000)
Alihe	Syenogranite (1)	160	2.91	710	Wu et al. (2000)
Hengdaohezi	Adamellite (1)	170	2.35	764	Wu et al. (2000)
Shimeng	Granodiorite (1)	245	0.44	980	Wu et al. (2000)
Tiangang	Monzogranite (2)	151	0.63	889	Wu et al. (2000)
Jiangmifeng	Diorite (1)	164	0.74	890	Wu et al. (2000)
Tianqiaogang	Syenogranite (2)	191	1.35–2.35	781–862	Wu et al. (2000)
Baishishan	Granodiorite (1)	196	1.64	843	Wu et al. (2000)
	Tonalite (1)	196	1.65	843	Wu et al. (2000)
Wujimi	Monzogranite (1)	185	2.09	798	Wu et al. (2000)
Dawangzhezi	Monzogranite (2)	183	3.21–3.96	643–704	Wu et al. (2000)
Yanshou	Granodiorite	195	1.75	833	Wu et al. (2000)
	Syenogranite	195	−0.81	1042	Wu et al. (2000)
Maojiatun	Alkaline granite (2)	210	0.23 to −1.42	968–1103	Wu et al. (2000)
Langxiang	Granodiorite (2)	206	−3.45–2.09	814–1265	Wu et al. (2000)
Milin	Alkaline granite (1)	200	−0.15	988	Wu et al. (2000)
Tuanjie	Granodiorite (1)	200	−0.38	1011	Wu et al. (2000)
Xiaobai	Monzogranite (2)	200	−0.08 to −1.20	986–1078	Wu et al. (2000)
Shichang	Granodiorite (2)	130	−2.12 to −2.86	1096–1156	Wu et al. (2000)
Qingshui	Alkaline granite (3)	170	−0.47 to −2.23	991–1137	Wu et al. (2000)
	Alkali feldspar granite (1)	170	−1.06	1041	Wu et al. (2000)
Dongqing	Granodiorite (2)	207	−0.46	1024	Wu et al. (2000)
	Monzogranite (1)	207	−0.77	1049	Wu et al. (2000)
	Syenogranite (1)	207	−1.91	1128	Wu et al. (2000)
Dongfengsuo	Syenogranite (1)	205	−6.27	1494	Wu et al. (2000)
	Alkaline granite (1)	205	−7.14	1563	Wu et al. (2000)
Chushan	Granodiorite (2)	253	−7.02 to −7.36	1591–1621	Wu et al. (2000)
Chaihe	Monzogranite (1)	254	−6.84	1581	Wu et al. (2000)
Wuoduhe	Granite (1)	127	−2.51	1137	Wu et al. (1999)
Xinhuatun	Granite (7)	165	2.06–2.81	723–782	Wu et al. (1999)
Lamashan	Granite (9)	150	120–1.53	809–842	Wu et al. (1999)
Yiershi	Granite (9)	145	1.86–2.48	733–783	Wu et al. (1999)
Duobaoshan	Granite Porphyry (3)	300	2.66–6.70	467–845	Wu et al. (1999)
Tongshan	Granite Porphyry (3)	300	3.56–7.11	483–744	Wu et al. (1999)
Baishilazi	Alkali feldspar granite (1)	123	2.01	752	Wu et al. (2002)
Xiaoshantun	Alkali feldspar granite (1)	285	2.62	835	Wu et al. (2002)
Guluhe	Alkali feldspar granite (1)	264	1.97	872	Wu et al. (2002)
Shangmachang	Alkali feldspar granite (2)	106	0.19–0.05	899–887	Wu et al. (2002)
Daheishan	Alkali feldspar granite (3)	292	4.24–5.34	620–710	Wu et al. (2002)
Songmushan	Alkali feldspar granite (1)	260	2.09	858	Wu et al. (2002)
Nianzishan	Syenite (1)	135	2.29	725	Li et al. (1994)
	Peralkaline granite (3)	118	2.55–2.83	682–704	Li et al. (1994)
	Basalt (1)	108	3.5	452	Li et al. (1994)
	Andesite	141	3.8	488	Li et al. (1994)
	Peralkaline granite (10)	125	0.89–4.29	569–847	Wei et al. (2001)
Changbaishan	Tholeiite (5)	18–2.12	−2.28–2.87	620–1030	Xie et al. (1992)

(*continued on next page*)

Table 1 (*continued*)

Location	Rock type (number of sample)	Age (Ma)	εNd(*T*)	T_{DM} (Ma)	Reference
	Trachyte (4)	0.6–0.2	−0.70–0.37	820–900	Xie et al. (1992)
Jingbohu	Basalt (4)	0.0–50	0.40–2.7	540–850	Liu et al. (1989)
Sikhote-Alin, Russia					
Dalinsky	Monzogranite (1)	103	0.04	900	Krimsky et al. (1998)
	Granodiorite (3)	100	−3.10 to −5.04	1150–1310	Krimsky et al. (1998)

Each subgroup of samples is listed roughly in geographic order from west to east, to emphasize geographic variation. The calculation of T_{DM} is based on two-stage model.

microcontinents and orogenic belt (Kovalenko et al., 1996a; Hong et al., 2000).

3. Phanerozoic granites with positive εNd values in the Central Asian Orogenic Belt and the Laurasia supercontinental cycle

However, such large-scale mantle-derived granites and volcanic rocks emplaced in the CAOB in the Phanerozoic could imply large-scale continental crustal growth during the Phanerozoic. The CAOB could be the most important area of continental crustal growth during the Paleozoic (Jahn et al., 2000a,b; Hong et al., 2000). Why does the largest area of granites in the world occur in central Asia? Why do the Phanerozoic granites with positive εNd values concentrate in the CAOB? And why has Central Asia become the most important belt for continental crustal growth worldwide in the Phanerozoic? We believe that it can be related to Laurasia supercontinental assembly, particularly in a region where plate tectonics was very intensive, and consuming plate boundaries were concentrated during Laurasia supercontinental assembly.

The sole, and commonly admitted supercontinent in the Phanerozoic, Pangea, comprised two contrasting supercontinents in shape and structure: an emergent southern supercontinent (Gondwanaland) was an entire and extensive continent from the early Paleozoic to Triassic, whereas simultaneously a submergent northern supercontinent (Laurasia) was amalgamated gradually with some continental blocks. The Hercynian collision of Gondwanaland and Laurasia marked the initial coalescence of Pangea in the mid-Carboniferous (320 Ma), which finally became a uniformly emergent supercontinent in the Triassic. Starting in the mid-Jurassic (160 Ma), Pangea broke up into fragments (Veevers, 1994). It follows that the most intensive tectonism occurred in the northern supercontinent (Laurasia) during Pangea supercontinental assembly. However, the tectonic evolution of the CAOB was just a key step leading to the formation of the Laurasia supercontinent.

It is worth considering that the peak of T_{DM} of granites are roughly consistent with the ages of the maximum opening of the Paleo-Asian ocean recorded by ancient ophiolite and island-arc complex (Hong et al., 2000). It follows that at least some of granites (for example, some of the early Paleozoic and early late-Paleozoic) could be related to subduction processes of the Paleo-Asian oceanic crust, and the source of the granites could be subducted oceanic crust and overlying metasomatized mantle wedge (Martin, 1986; Defant and Drummond, 1990). Whereas, the extensive late Paleozoic and Mesozoic granites could be formed by partial melting of juvenile continental crust resulting from subducted oceanic crust at 800–600 Ma within a large-scale extensional regime induced after the Devonian-Carboniferous collision between the Siberian and Sino-Korean-Tarim plates, which provided the condition for underplating of the mantle-derived materials and delamination of lithosphere mantle (Hong et al., 2000). In other words, the Phanerozoic granites in the CAOB formed during the course of subduction and collision and in an extensional regime after the collision, which suggests that the formation of the granites with positive εNd values in the CAOB was closely related temporally and spatially to Laurasia supercontinental assembly and breakup and dispersal.

Engebreston et al. (1992) calculated the amounts and positions of subducted-accumulated oceanic lithospheres

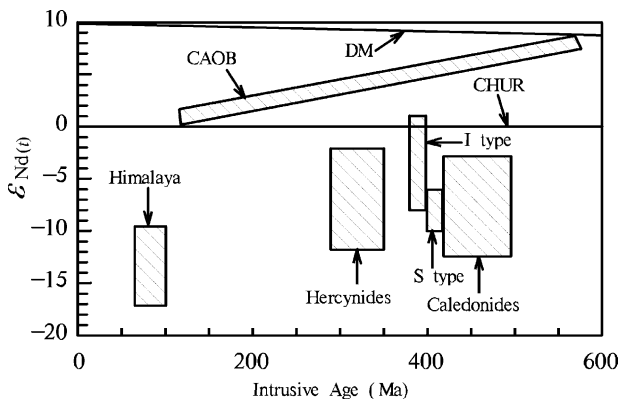

Fig. 3. εNd(*T*) vs intrusive age plot for Phanerozoic granites. Data from the following areas: CAOB, from Hong et al. (2000); Caledonides, Hercynides and Himalaya from Patchett (1992); S- and I- type granites from the Lachlan fold belt, Australia from McCulloch and Chapell (1982).

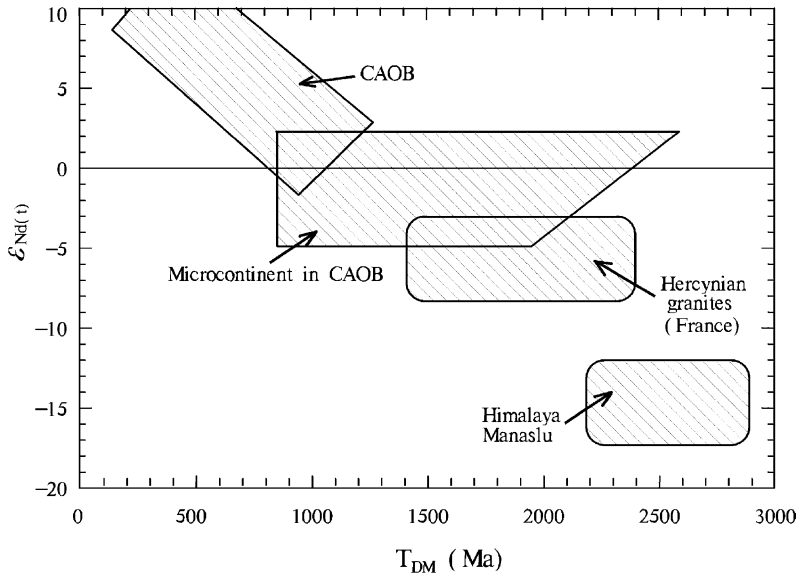

Fig. 4. Plot of εNd(T) vs T_{DM} of granites. CAOB and microcontinent in CAOB from Hong et al. (2000); Hercynian granites in French from Bernard-Griffiths et al. (1985); Downes et al. (1997); Himalayan granites from Vidal et al. (1984).

for the last 180 Ma with magnetic strips in the hotspot framework under the assumption that the hot-spots on the plates have been immobile with respect to the deeper mantle during the last 180 Ma, and they showed that the largest amount of subducted slabs with more than 8000 km length for the last 180 Ma were situated under Central Asia. Recent results from global seismic tomography (Fukao et al., 1994; Grand et al., 1997; Van der Voo et al., 1999; van der Hilst and Karason, 1999) indicated that *P*-wave high-velocity anomalies are distributed in good agreement with the calculated positions of subducted slabs by Engebreston et al. (1992). Such a spatially restricted distribution implies that the high-*V* anomalies mark the sites of subducted-accumulated oceanic lithospheres at consuming plate boundaries during the last 180 Ma, which Engebreston et al. (1992) called lithospheric graveyards.

But the high-*V* anomaly just above the Core–Mantle Boundary (CMB) under Central Asia appears to be too wide, as compared with the overlying high-*V* anomaly at a depth 700–1700 km and with the calculated amounts of subducted slabs for the last 180 Ma. It seems to be difficult to explain in terms of the subduction history in the last 180 Ma. To explain the anomaly in this region, the subduction history has to be traced back to much older times. In fact, the anomalously high-*V* area above the CMB roughly coincides with the region in which consuming plate boundaries during the Permian, Triassic, and Jurassic times are concentrated (Fukao et al., 1994). Moreover, based on geological and paleomagnetic data, the Siberian platform situated mainly on medium and high latitudes in the North Hemisphere during the Phanerozoic, and experienced only a clock-wise rotation in situ, without any significant drift (Yarmolyuk et al., 2000; Kovalenko et al., 2002). Thus, the largest mass of high-*V* anomaly on the CMB underneath Asia may represent in part the subducted and accumulated slabs before the collision–amalgamation of Asia, although it is difficult to make a quantitative estimate for the amount of subducted slabs before 200 Ma (Fukao et al., 1994).

Interestingly, the largest mass of high-*V* anomaly underneath Asia also coincides in space with the distribution of the granites with positive εNd values in the CAOB. These facts suggest that eastern Asia had been a region in which plate tectonics was very intensive, and collision–amalgamation between continental blocks occurred in multiple phase at least since 300 Ma, resulting in the large amount of oceanic slabs subducted beneath Asia during the formation of Asia before 300–200 Ma, hence inducing extensive mantle-derived magmas, voluminous granites with positive εNd values, and the large-scale continental crustal growth in the area. In fact, the sites of crustal growth in the history of the earth usually occur along well-defined belts, preferentially along subduction zones or paleosubduction zones (Boher et al., 1992; Albarede, 1998).

In addition, the Pangea supercontinental cycle was accompanied by global mass extinction events of the biosphere, anoxic events, sea-level changes and climatic changes at the end of the Permian (Veevers, 1994). It is possible that during Pangea supercontinental assembly, subduction of old oceanic crust was at a maximum, leading to an increase in arc volcanism to influence the major geochemical cycles both elemental and isotopic. Moreover, the continental collision that terminated the assembly process would promote crustal thickening, intracrustal melting and differentiation of lithospheric mantle, resulting in large-scale post-orogenic magmatism, and leading to global anoxia, climatic changes, sea-level changes and mass extinction events.

4. Discussion

Another interesting question, although somewhat peripheral to this paper, is that inasmuch as the episodes of crustal growth appear to correlate reasonably well with supercontinental assembly, supercontinental breakup and dispersal cannot be accompanied by large-scale continental growth. But the latter is frequently accompanied by outpourings of continental plateau and flood basaltic lava, and formation of oceanic plateaus, in order to maintain a steady state system during supercontinental breakup and dispersal, these process are necessarily accompanied by the continental crustal losses recycled through the mantle, such that new additions of the crust are balanced by losses. For example, the Dupal anomaly, a large-scale Pb isotopic anomaly, forming a globe-encircling belt in the Southern Hemisphere centred today on latitude 30°S (Dupre and Allegre, 1983; Hart, 1984), could be the result of recycling of the crust into the mantle during the breakup and dispersal of Gondwanland and the opening of the South Atlantic and Indian oceans since the mid-Jurassic (160 Ma), leading to the changes of mantle composition (Anderson, 1985; Hawkesworth et al., 1986; Condie, 2000). Because OIB with Pb isotopic anomaly in geological history would have been entrained in subduction zones with sea-floor spreading and finally subducted beneath continents into the mantle, they could not be preserved. Similarly, the fact that Mesozoic granites later than 200 Ma in CAOB are characterized by εNd values approaching zero, could be a result of the enhancement of continental crustal recycling during the Pangea supercontinental breakup and dispersal.

Therefore, the evolution of continental crust is accompanied not only by assembly and breakup of a supercontinent, but also by growth and loss (recycling) of the crust with regard to the Laurasia supercontinent. If the large-scale Phanerozoic growth of the crust in the CAOB is accepted, the production rate of continental crust must significantly exceed the recycling rate at these time. During the formation of a supercontinent, the production rate of oceanic crust, the subduction rate and hence the production rate of juvenile continental crust in arc systems should be increased due to increased convection rate or/and increase of the total length of the ocean ridge system (Larson, 1991). The breakup and dispersal of a supercontinent is accompanied not only by the continental crustal growth resulted by outpouring of plateau and flood basalts, and formation of oceanic plateaus, but also by the enhanced recycling of the crust resulted from more perimeter per-unit-volume and more rivers entering the ocean per-unit-length of continent perimeter in smaller fragments than in the same volume of a supercontinent (Condie, 2000), resulting in a steady state system. Therefore, the time periods when large areas of continental crust were rapidly formed during supercontinent assembly alternate with apparently more quiescent periods of low-crust-forming rates during supercontinental breakup and dispersal, which is roughly demonstrated by a stair-case pattern of crustal growth (Fig. 1). The continents are now approaching their maximum dispersal (Hoffman, 1992), hence continental crustal growth is basically in steady state (Larson, 1991). If a period of supercontinental cycle was at 0.4–0.5 Ga (Nance et al., 1988), a future supercontinent could be formed 250 Ma after present (Maruyama, 1994), and then continental crustal growth should continue.

5. The mechanics of a supercontinental cycle and continental crustal growth

Most models for the mechanics of a supercontinental cycle and continental crustal growth advocate that episodic instability at the 660 km seismic discontinuity may control either the growth of continental crust (Stein and Hofmann, 1994; Bruer and Spohn, 1995), or a supercontinental cycle (Fukao et al., 1994; Maruyama, 1994; Peltier et al., 1997). Subducted slabs tend to stagnate at the 660 km discontinuity until the volume reaches a critical value to cause catastrophical gravitational fall into the lower mantle (slab avalanche), and convection patterns change in the mantle from layered convection to whole-mantle convection in short-lived episodes. When the slabs arrive at the D″ layer above the core, they are heated to generate large plumes that ascend rapidly to the base of the lithosphere, where they are responsible either for crustal growth or supercontinental breakup and dispersal. Condie (1998, 2000) suggested that slab avalanche events in the mantle correlate with major episodes of crustal formation, whereas the supercontinental cycle probably operates independently of slab avalanches.

If the above proposed scenario about the Phanerozoic granites with positive εNd in the CAOB and Laurasia supercontinent is correct, a model that ties together catastrophic slab avalanches in the mantle, the supercontinental cycle and episodic production of continental crust is presented as follows (Fig. 5), which is in large part highly speculative. Since the Mid-Proterozoic, the breakup and dispersal of supercontinents accompanied new additions of the crust balanced by losses, resulting in a steady state system, and triggered a catastrophic collapse of subducted slabs that accumulated at the 660 km seismic discontinuity (slab avalanche), resulting in cold mantle downwelling and changing mantle convection from layered to whole mantle (Fukao et al., 1994; Maruyama, 1994; Stein and Hofmann, 1994). Continental fragments may be swept toward convective downwelling where they reaggregate, thus leading to the formation of a supercontinent (Hoffman, 1989; Maruyama, 1994; Peltier et al., 1997). Supercontinent assembly accompanied by large-scale subduction, collision and an extensional regime after collision, results in transfer of mantle-derived magmas into the crust, and the production rate of juvenile crust could significantly exceed the recycling rate, hence inducing obviously continental crustal growth. During the assembly phase, mantle convection

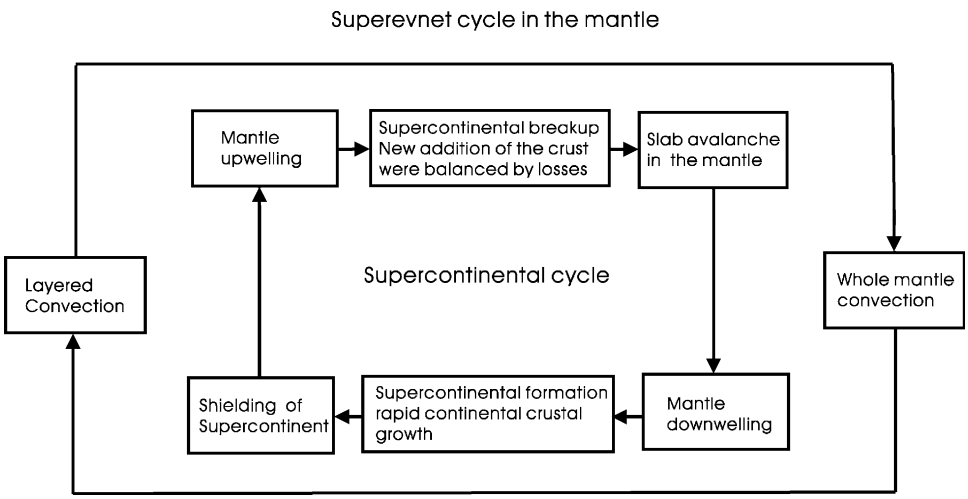

Fig. 5. The supercontinental cycle and superevent cycle modified after Condie (1998, 2000).

patterns transfer back from whole to two-layer mantle. The thermal shielding of a large volume of mantle from the cooling effect of subduction beneath supercontinents can result in the production of mantle upwellings that eventually break up supercontinents (Gurnis, 1988; Hoffman, 1989; Fukao et al., 1994).

6. Conclusions and speculations

Contrasting sharply with other Phanerozoic crust-derived granites with negative εNd values over the world, the Paleozoic-Mesozoic granites in the CAOB have commonly positive εNd values, implying a large-scale continental crustal growth in the Phanerozoic. They coincided temporally and spatially with the Phanerozoic Pangea supercontinental cycle (320–250 Ma), and overlapped in space with the *P*-wave high-*V* anomalies and calculated sites of subducted slabs for the last 180 Ma, which suggests that the Phanerozoic Laurasia supercontinent assembly was accompanied by large-scale continental crustal growth in central Asia. The latter occurred along well defined belts in which plate tectonics was very intensive, collision–amalgamation between continents occurred in multiple phases, and consuming plate boundaries were concentrated during supercontinent assembly.

If this is the case, a model is presented here that rapid continental crustal growth occurred during supercontinental assembly, whereas new addition of the crust were balanced by losses, resulting in a steady state system during supercontinental breakup and dispersal. The supercontinental cycle and continental crustal growth are both governed by changing patterns of mantle convection.

Acknowledgements

We would like to thank Prof. B.M. Jahn for stimulating this contribution, and we acknowledge Prof. K.C. Condie and Prof. B.F. Windley for their constructive criticism that helped greatly in improving the paper. The work is financially supported by Major State Basic Research Program of People/s Republic of China (No. 2001CB409800), National Natural Science Foundation of China (Grand No. 49772105 and 40072023) and china Geological Survey Project No. 200113900018".

References

Albarede, F., 1998. The growth of continental crust. Tectonophysics 296, 1–14.

Anderson, D.L., 1985. Hotspot magmas can form by fractionation and contamination of mid-ocean ridge basalts. Nature 318, 145–149.

Armstrong, R.L., 1968. A model for Sr and Pb isotope evolution in a dynamic Earth. Rev. Geophys. 6, 175–199.

Bernard-Griffiths, J., Peucat, J.J., Sheppard, S., Vidal, P., 1985. Petrogenesics of Hercynian leucogranites from the southern Armorican Massif: contribution of REE and isotopic (Sr, Nd, Pb and O) geochemical data to the study of source rock characteristics and ages. Earth Planet Sci. Lett. 74, 235–250.

Boher, M., Abouchami, W., Michard, A., Albarede, J., Arndt, N.T., 1992. Crustal growth in West-Africa at 2.1 Ga. J. Geophys. Res. 97, 345–369.

Bowring, S.A., Housh, T., 1995. The Earth's early evolution. Science 269, 1535–1540.

Bruer, D., Spohn, T., 1995. Possible flush instability in mantle convection at the Archean-Peoterozoic transition. Nature 378, 608–610.

Chen, Y. X., Chen, W. J., Zhou, X. H., Li, Q., Zhang, G H., Chen, S. H., 1997. Mesozoic volcanic rocks in west Liaoning province and the surroundhrg regions: Geochronology, Geochemistry and Tectonic setting. Seismological Press, Beijing, 279pp, in Chinese.

Chen J., Man F., Ni S., 1995. Neodymium and strontium isotopic geochemistry of mafic- ultramafic intrusions from Qinbulake rock belt, west Tianshan mountain, Xinjiang. Geochemistry, 24(2), 121–127, in Chinese with English abstract.

Chen, B., Jahn, B. M., Wilde, S., Xu, B., 2000. Two contrasting Paleozoic magmatic belts in northern Inner Mongolia, China: petrogenesis and tectonic implications. Tectonophysics, 328, 157–182.

Chen, B., Jahn, B.-m., Wang, Shiguang, 2001. Nd isotopic Characteristics of the Paleozoic meta-Sedimentary rocks from Altai, Xinjiang, China

and their constraint on crustal evolution. Science in China (series D), 31 (3), 226–232, in Chinese.

Condie, K.C., 1998. Episodic continental growth and supercontinents: a mantle avalanche connection? Earth Planet Sci. Lett. 163, 97–108.

Condie, K.C., 2000. Episodic continental growth models: afterthoughts and extensions. Tectonophysics 322, 153–162.

Defant, M.J., Drummond, M.S., 1990. Derivation of some modern arc magmas by melting of young subducted lithosphere. Nature 347, 662–665.

De Paolo, D.J., 1981. A Nd and Sr isotopic study of the Mesozoic calealkaline granitic batholiths of the Sierra Nevada and Peninsular Range, California. J. Geophys. Res. 86, 10470–10488.

Dobretsov, N.L., Berzin, N.A., Buslov, M.M., 1995. Opening and tectonic evolution of the Paleo-Asian ocean. Int. Geol. Rev. 37, 335–360.

Downes, H., Shaw, A., Williamson, B.J., Thirlwall, M.F., 1997. Sr, Nd and Pb isotope geochemistry of the Hercynian granodiorites and monzogranites, Massif Central, France. Chem. Geol. 136, 99–122.

Dupre, B., Allegre, C., 1983. Pb–Sr isotope variation in Indian Ocean basalts and mixing phenomena. Nature 303, 142–146.

Engebreston, D.C., Kelley, K.P., Cashman, H.J., Richards, M.A., 1992. 180 million years of subduction. GSA Today 2, 93–95.See also page 100.

Fukao, Y., Maruyama, S., Obayashi, M., Inoue, H., 1994. Geologic implication of the whole mantle *P*-wave tomography. J. Geol. Soc. Jpn 100 (1), 4–23.

Grand, S.P., van der Hilst, R.D., Widiyantoro, S., 1997. Global seismic tomography: a snapshot of convection in the earth. GSA Today 7 (4), 1–7.

Gurnis, M., 1988. Large scale mantle convection and aggregation and dispersal of supercontinents. Nature 332, 695–699.

Hart, S.R., 1984. A large-scale isotope anomaly in the Southern Hemisphere mantle. Nature 309, 753–757.

Han, B., Wang, S., Jahn, B.-m., Hong, D., Kagami, H., Sun, Y.-l., 1997. Depleted-mantle source for the Ulungur River A-type granites from North Xinjiang, China: geochemistry and Nd-Sr isotopic evidence, and implications for Phanerozoic crustal growth. Chemical Geology. 138, 135–159.

Han B., Wang S., Sun Y., Hong D., 1998. Subaluminium-peraluminium granites with positive εNd (T) values of Yebushan pluton, Xin]iang. Chinese Sci. Bull., 43 (12), 1323–1328, in Chinese.

Hawkesworth, C.J., Mantovani, M.S.M., Taylor, P.N., Palacz, Z., 1986. Evidence from the Parana of south Brazil for a continental contribution to Dupal Basalts. Nature 322, 356–358.

He B., Tan K., Wu Q., 1994. Ages and Sr, Nd isotopic evidences of mantle source magmatite in the Bu's gold deposit, Jimunai, northern Xinjiang. Geotectonica et Metallogenia. 18,219–228, in Chinese with English abstract.

Heinhorst, J., Lehmann, B., Ermolov, P., Serykh, V., Zhurutin, S., 2000. Paleozoic crustal growth and metallogeny of Central Asia: evidence from magmatic-hydrothermal ore systems of Central Kazakhstan. Tectonophysics, 328,69–87.

Hildreth, W., Moorbath, S., 1988. Crustal contributions to arc magmatism in the Andes of Central Chile. Contrib. Miner. Petrol. 98, 455–489.

Hoffman, P.F., 1989. Speculations on Laurentia's first gigayear (2.0 to 1.0 Ga). Geology 17, 135–138.

Hoffman, P.F., 1992. Supercontinents, Encyclopedia of Earth System Science, V. 4, Academic, Sandiego, CA, pp. 323–328.

Hong, D., Wang, S., Xie, X., Zhang, J., 2000. Genesis of positive εNd granitoids in the Da Hinggar Mts-Mongolia orogenic belt and continental crustal growth. Earth Sci. Frontiers 7, 441–456, in Chinese.

Hong, D., Wang, S., Xie, X., Zhang, J., 2001. The Phanerozoic continental growth in Central Asia and the evolution of Laurasia supercontinent. Gondawana Res. 4, 632–633.

Hopson, C., Wen, J., Tilton, G., Tang, Y., Zhu, B., Zhao, M., 1989. Paleozoic Plutonism in East Junggar, Bogdashan and eastern Tianshan, NW China. EOS, 70 (43), 1403–1404.

Huang X., Jin C., Sun B., Pan J., Zhang R., 1997. Study on the age of Armantai ophiolite, Xinjiang by Nd-Sr isotopic geology. Acta Petrologica Sinica, 13,85–91, in Chinese with English abstract.

Jahn, B.M., Wu, F., Hong, D., 2000a. Important crustal growth in the Phanerozoic: isotopic evidence of granitoids from east-central Asia. Proc. Indian Acad. Sci. (Earth Planet Sci. 109 (1), 5–20.

Jahn, B.M., Wu, F., Chen, B., 2000b. Masssive granitoid generation in central Asia: Nd isotopic evidence and implication for continental growth in the Phanerozoic. Episodes 23, 82–92.

Kepezhinskas, P. K., Kepezhinskas, K. B., Pukhtel, I. S., 1991. Lower Paleozoic Oceanic Crust in Mongolian Caledonides: Sm-Nd Isotope and Trace Element Data. Geophysical Research Letters, 18 (7), 1301–1304.

Khain, E.V., Bibikova, E.V., Kroner, A., Zhuralev, D.Z., Sklyarov, E.V., Fedotova, A.A., Kravchenko-Berezhnoy, I.R., 2002. The most ancient ophiolite of the Central Asian fold belt: U–Pb and Pb–Pb zircon ages for the Dunzhugur Comples, Eastern Sayan, Siberia, and geodynamic implications. Earth Planet Sci. Lett. 199, 311–325.

Kovalentko, V. I., Tsareva, G M., Yarmolyuk, V. V., Troitsky, V. A., Farmer, J. L., Tshernishev, I. V., 1992. Sr and Nd isotopic composition and ages of bearing rare metal granitoids, western Mongolia. Rep. Acad. Sci., 327 (4–6) 570–574, in Russian.

Kovalenko, V.I., Yarmolyuk, V.V., Kovach, V.P., Kotov, A.B., Kozakov, I.K., Salnikova, E.B., 1996a. Sources of Phanerozoic granitoids in Central Asia: Sm–Nd isotope Data. Geochemistry 8, 699–712, in Russian.

Kovalentko, V. I., Yarmolyuk, V. V., Puhtel, I. S., Stash, K. H., Yagutts, E., Korikovsky, S. P., 1996b. Magmatic rocks and sources of magma of ophiolite, Lake area, Mongolia. Petrology, 4 (5), 453–495, in Russian.

Kovalentko, V. I., Kostitsyn, Yu, A., Yarmolyuk, V V., Budnikov, S. V., Kovach, V. P., Kotov, A. B., Salnikova, E. B., Antipin, V. S., 1999. Sources of magma and Sr, Nd isotopic evolution of bearing rare metal Li-F granitoids. Petrology, 7 (4), 401–429, in Russian.

Kovalenko, V.I., Yarmolyuk, V.V., Vladikin, N.V., Ivanov, V.G., Kovach, V.P., Kozlovsky, A.M., Kostitisin, Yu.A., Kotov, A.B., Salnikova, E.B., 2002. Epoch of formation, geodynamic setting and sources of bearing rare metal magmatism in Central Asia. Petrology 10 (3), 227–253, in Russian.

Kozakov, I. K., Kotov, A. B., Kovach, V. P., Salnikova, E. B., 1997. Crustal-forming process during the geological evolution of Baidarik block, central Mongolia. Petrology, 5 (3), 227–235, in Russian.

Krimsky, R. Sh, P., V. A., Rub, M. G, Belyatsky, B. V., Levcky, L. K., 1998. Rb-Sr and Sm-Nd isotope characteristics of granitoids and scheelite mineral deposits, Vostok-2, Coastal Area. Petrology, 6 (l), 3–15, in Russian.

Kruk, N. N., Rudnev, S. N., Vladimirov, A. G, Zhuravlev, D. Z., 1999. Sm-Nd isotopic system of the granitoids in western Altai-Sayan folding area. Rep. Acad. Sci., 336 (3), 226–232, in Russian.

Kwon, S. T., Tilton, G R., Coleman, R. G, Feng, Y., 1989. Isotopic studies bearing on the tectonics of the west Junggar region, Xinjang, China. Tectonics, 8,719–729.

Larson, R.L., 1991. Latest pulse of Earth: evidence for a mid-Cretaceous superplume. Geology 19, 547–550.

Li, P. Z., Yu, J. S., 1994. Isotopic geochemistry of Nianzishan miarolitic granite, In: Chen, H. S. ed. Isotopic Geochemical Research. Zhejiang University Press, Hangzhou, pp. 269–286, in Chinese.

Li, H., et al., 1998. Study on Metallogenetic Chronology of Nonferrous and Precious Metallic Ore Deposits in North Xinjiang, China, Geological Publication House, Beijing, 263 p, in Chinese with English abstract.

Liu B., Chen X., Zhu B., 1989. Origin of Cenozoic basalts from Jinbohu, Northeast China and chemical characteristics of their mantle source—Sr-Pb isotopic and trace element evidence. Geochemica, 1,9–19, in Chinese with English abstract.

Martin, H., 1986. Effect of steeper Archean geothermal gradient on geochemistry of subduction zone magmas. Geology 14, 753–756.

Maruyama, S., 1994. Plume tectonics. J. Geod. Soc. Jpn 100 (1), 24–49.

McCulloch, M.T., Chappell, B.W., 1982. Nd isotopic characteristics of S- and I-type granites. Earth Planet. Sci. Lett. 58, 51–64.

McCulloch, M.T., Bennett, V.C., 1994. Progressive growth of the earth's continental crust and depleted mantle: Geochemical constraints. Geochim. Cosmochim. 58, 4717–4738.

Nance, R.D., Worsley, T.R., Moody, J.B., 1988. The supercontinent cycle. Sci. Am. 256 (July), 72–79.

Ni S., Man F., Chen J., 1994. Sm-Nd isotope ages of basic and ultrabasic rocks from the Qingbulak belt, Xinjiang. Acta Petrol. et Mineral., 13 (3), 227–231, in Chinese with English abstract.

Patchett, P.J., 1992. Isotopic studies of Proterozoic crustal growth and evolution. In: Condie, K.C., (Ed.), Proterozoic crustal evolution, Elsevier, Amsterdam, pp. 481–508.

Peltier, W.R., Butler, S.P., Solheim, L.P., 1997. The influence of phase transformations on mantle mixing and plate tectonics. In: Crossley, D.J., (Ed.), Earth's deep interior, Gordon & Breach, Amsterdam, pp. 405–430.

Rui, Z., Liu Y., Wang L., Wang Y., 2002. The eastern Tianshan porphyry copper belt in Xinjiang and its tectonic framework. Acta Geologica Sinica, 76, 83–94, in Chinese with English abstract.

Shao, J., Zhang L., Mu B., 1999. Magmatism in the Mesozoic extending erogenic process of Da Hinggan MTS. Earth Science Frontiers, 6, 339–346, in Chinese with English abstract.

Stein, M., Hofmann, A.W., 1994. Mantle plumes and episodic crustal growth. Nature 372, 63–68.

Sun M., Zhang L., Yuan C., 1998. Mela-enclaves and their host A-tyge granites in western Junggar, China: a geochemical study. In: John Borruing and Hong Dawei eds. IGCP-420 Project First Workshop abstract, Urumqi, Xinjiang, China. P. 37, in Chinese with English abstract.

Taylor, S.R., McLennan, S.M., 1995. The geochemical evolution of the continental crust. Rev. Geophys. 33, 241–265.

Van der Hilst, R.D., Karason, H., 1999. Compositional heterogeneity in the bottom 1000 kilometers of earth's mantle: toward a hybrid convection model. Science 283, 1885–1888.

Van der Voo, R., Sparkman, W., Bijwaard, H., 1999. Mesozoic subducted slabs under Siberia. Nature 397, 246–249.

Veevers, J.J., 1994. Pangea: evolution of a supercontinent and its consequences for Earth's paleoclimate and sedimentary environments. In: Klein, G.D., (Ed.), Pangea, Paleoclimate, Tectonics, and Sedimentation during Accretion, Zenith, and Breakup of a Supercontinent, 288. Geological Society of America Special Paper, Boulder, CO, pp. 13–23.

Vidal, P., Bernard-Griffiths, J., Cocherie, A., Le Fort, P., Peucat, J.J., Sheppard, S., 1984. Geochemical comparison between Himalayan and Hercynian leucogranites. Phys. Earth Planet Interiors 35, 179–190.

Vladimirov, A. G, Vystavnoi, S. A., Titov, A. V., Rudnev, S. N., Dergachev, V. B., Annikov, I. Yu., Tikunov, Yu. V., 1998. Petrology of the early Mesozoic rare-metal granites of the southern Gorny Altai. Geol. and Geophys. 39 (7), 901–916, in Russian.

Vorontsov, A. A., Yarmolyuk, V. V., Ivanov, V. G, Nikiforov, A. V., 2001. Late Mesozoic magmatism of Dzhiginsk segment, western Transbaikalia rift area: Stage of formation, association and sources. Petrology, 10 (5), 510–531, in Russian.

Wang Y., Zhao Z., 1997. Geochemistry and origin of the Baerzhe REE-Nd-Be-Zr superlarge deposit. Geochemica, 26,24–35, in Chinese with English abstract.

Wang T., Zheng Y., Li T., Gao Y., 2004. Phanerozoic continental growth in Central Asia. Journal of Asian Earth Sciences, this assure.

Wei C., Zheng Y., Zhao Z., 2001. Nd-Sr-O isotopic geochemistry constrains on the age and origin of the A-type granites in eastern China. Acta Petrologica Sinica, 17, 95–111, in Chinese with English abstract.

Wu F., Song D., Lin Q., 1999. Petrogenesis of the Phanerozoic granites and crustal growth in Northeast China. Acta Petrologica Sinica, 15, 181–189, in Chinese with English abstract.

Wu F., Jahn, B.-m., Wilde, S., Sun, D., 2000. Phanerozoic crustal growth: U-Pb and Sr-Nd isotopic evidence from the granites in northeastern China. Tectonophysics, 328, 89–113.

Wu F., Sun, D., Li, H., Jahn, B.-m., Wilde, S.2002. A-type granites in northeastern China: age and geochemical constraints on their petrogenesis. Chemical Geology, 187, 143–173.

Xie G., Wang J., 1992. Geochemical study of Cenozoic volcanic rocks in Changbaishan area. In: Liu Ruoxin ed. Geochronology and geochemistry of the Cenozoic volcanic rocks in China. Seismological Press, Beijing, pp. 201–212, in Chinese.

Yarmolyuk, V. V., Kovalentko, V. I., Ivanov, V. G, Zhuravlev, D. Z., 1995. Sr and Nd isotopic composition of basic volcanic rocks in south Hangai hotspot, aentral Asia. Rep. Acad. Sci., 342 (2), 230–234, in Russian.

Yarmolyuk, V. V., Vorontsov, V. L., Kovalentko, V. I., Zhuravlev, D. Z., 1997. Isotopic inhomogeneity of sources of late Paleozoic intraplate magmatism in central Asia. Geol. and Geophys. 38 (6), 1142–1147, in Russian.

Yarmolyuk, V. V., Ivanov, V. G, Kovalentko, V. I., 1998. Sources of the late Mesozoic-Cenozoic intraplate magmatism in western Transbailia. Petrology, 6 (2), 115–138, in Russian.

Yarmolyuk, V.V., Kovalenko, V.I., Kuzmin, M.I., 2000. North Asia superplume in the Phanerozoic: magmatism and geodynamics. Geotectonics 5, 3–29, in Russian with English abstract.

Yarmolyuk, V. V., Litivinovsky, B. A., Kovalentko, V. I., Jahn, Borming, Z., A. N., Vorontsov, A. A., Zhuravlev, D. Z., Posohov, V. F., Kuzmin, D. V, Sangimirova, G P., 2001. Stage of formation and sources of the Permian-Triassic alkaline granites in North Mongolia-Transbaikalia rift belt. Petrology, 9 (4), 351–380, in Russian.

Zhao, Z., Wang Z., Zou, T., Masuda, A., 1993. The REE, isotopic composition of O, Pb, Sr and Nd and digenetic model of granitoids in Altai region. In: G C..Tu ed. New Improvement of Solid Geosciences in northern Xinjiang, Science Press, Beijing, 239–266, in Chinese.

Zhao Z., Wang Z., Zou T., Masuda, A., 1996. Study on petrogenesis of Alkali-rich intrusive rocks of Ulungur, Xinjiang. Geochemistry, 25 (3), 205–220, in Chinese with English abstract.

Zhou T., Chen J., Li X., 1996. Origin of high εNd (t) granites from Alatao mountains, Xinjiang. Scien. Geol. Sinica, 31(l), 71–79, in Chinese with English abstract.

Zhu,Y., Sun, S., Jiang, N., 2001. A Cold-bearing Alkaline Pluton in Eastern Linxi District, Inner Mongolia: Its Geochemistry and Metallogenic Significance. Resource Geology, 51 (4), 393–399.